Songklanakarin J. Sci. Technol.
44 (3), 653-661, May - Jun. 2022

http://www.sjst.psu.ac.th

Original Article

Numerical analysis of unsteady non-Newtonian MHD nanofluid flow over a stretching sheet

Kharabela Swain[1*], Madhusudan Senapati[2], and Sampada Kumar Parida[2]

[1] *Department of Mathematics, Gandhi Institute for Technology, Bhubaneswar, 752054 India*

[2] *Department of Mathematics, Siksha 'O' Anusandhan (Deemed to be University), Bhubaneswar, Odisha, 751030 India*

Received: 29 July 2021; Revised: 11 October 2021; Accepted: 26 November 2021

Abstract

The advancement in the process of heating/cooling leads to a saving in energy, time, and life expectancy of the equipment. The effective heat transport can likewise be improved by increasing the thermal conductivity of the regular liquid. The current study explores the Brownian movement and thermophoresis on unsteady, radiative Casson magneto-nonoliquid stagnation point flow over a stretching sheet saturated in a porous medium in the presence of exponential space-based heat source/sink (ESHS). The resultant non-linear ordinary differential equations (ODEs) are solved by Runge-Kutta fourth order method with shooting technique. The significant results of the study presented through figures and tables. It is found that the more of Casson fluidity enhances the momentum diffusion in the flow domain and reduces the thermal and mass diffusion processes. The temperature distribution exceeds the prescribed temperature at the plate surface for higher diffusion. Hence, care should be taken to regulate the thermal diffusion to avoid the thermal instability.

Keywords: casson nonoliquid**,** stagnation point flow, Brownian movement, thermophoresis, thermal radiation, porous medium

1. Introduction

The heat transfer efficacy of the regular fluids can be improved by increasing the thermal conductivity of the fluids which is very vital for industrial applications. Commonly used fluids such as water, ethylene glycol, kerosene etc. have relatively low thermal conductivity, when compared to the thermal conductivity of solids. Nanofluid is a kind of heat transfer medium, containing nanoparticles (high dispersibility with predominant Brownian movement of the particles and radius <100 nm) which are uniformly and stably distributed in a base fluid. Choi (1995) established that thermal conductivities of fluids are greatly enhanced by the addition of nanoparticles. Buongiorno (2006) found that the Brownian movement and thermophoresis mechanisms are responsible for advancement in the thermal conductivity of nanoliquid.

*Corresponding author
Email address: kharabela1983@gmail.com

The non-Newtonian fluid, Casson fluid for example tomato sauce, honey, soup, orange juice and human blood, behave like an elastic solid at low shear stress and above a critical stress value; it behaves like a Newtonian fluid. Casson fluid is an ideal fluid model to represent the flow of blood in thin arteries. Further, MHD flow and heat transfer of Casson fluid in a saturated porous medium finds wide applications in polymer industry and biological system. Casson (1959) initially studied an experiential model to describe the flow curves of suspensions of pigments in lithographic varnishes used for preparation of printing inks. The non-Newtonian behaviour of blood, due to yield stress, lies between 0.01 and 0.06 dyn/cm^2, was studied by Krishnan, Rittgers, and Yoganathan (2012). Oyelakin, Mondal, and Sibanda (2016) studied the radiative Casson nanofluid over a stretching sheet. El-Aziz and Afify (2019a) explored the slip flow analysis of Casson nanofluid over a stretching sheet with Hall current effect. Many researchers (Abel, Mahesha, & Tawade, 2009; Bhandari, 2019; Das, Duari, & Kundu, 2014; Das, Mahanta, Shaw, & Parida, 2019; Goyal, & Bhargava, 2018; Hsiao, 2016; Pal, Mandal, & Vajravalu, 2015; Ibrahim, 2015;

Ibrahim, Kumar, Lorenzini, & Lorenzini, 2019; Reddy, Padma, & Shankar, 2015; Rout & Mishra, 2018; Senapati, Parida, Swain, & Ibrahim, 2020) studied the Casson nanofluid by considering different flow models. El-Aziz and Afify (2019b) explored the Hall current effect on Casson fluid flow over a stretching sheet. Reddy, and Chamkha (2016) examined the Soret and Dufour impacts on MHD flow of water based Al_2O_3 and TiO_2 nanofluids over a stretching sheet. Further, Daniel, Aziz, Ismail, and Salah (2019), Sreedevi, Reddy, and Chamkha (2020) analyzed the unsteady flow of radiative nanofluid over a stretching sheet. Seyedi, Saray, and Chamkha (2020) studied the Eyring-Powell flow over a stretching channel with chemical reaction.

The flow over a stretching sheet in a porous medium has numerous engineering applications in glass fiber, plasma studies, and geothermal energy extraction etc. with magnetic fields. For the appropriate cooling purpose, the higher thermal conductivity and better heat transmission rate are only possible, if the flow phenomena would be considered subjected to magnetic field. Several investigations were carried out by Chamkha (1997a); Chamkha (1997b); Chamkha (2000); Chamkha, Dogonchi, and Ganji (2019); Chamkha, and Khaled (2000); Chamkha, and Mohamed (2011); Ganesh, Reddy, Sudharani, Shehzad, and Chamkha (2020); Khedr, Chamkha, and Bayomi (2009); Takhar, Chamkha, and Nath (1999); Wakif, Chamkha, Animasaun, Zaydan, Waqas, and Sehaqui (2020) on the field of MHD fluid flow by taking different thermo-physical properties. Hall current and ion-slip currents with heat transfer have numerious industrial applications in power generators, MHD accelerators, refrigerators, electric transformers etc. Takhar, Chamkha, and Nath (2002), Krishna, and Chamkha (2019) have studied the Hall and ion slip effects on MHD rotating flow of nanofluid past a moving plate and an infinite vertical plate respectively in a porous medium. Krishna, Ahamad, and Chamkha (2020), Krishna, Ahamad, and Chamkha (2021), Krishna, and Chamkha (2020) and have examined the influences of Hall and ion slip on MHD rotating flow of elastic-viscous fluid and second grade fluid respectively. Modather, Rashad, and Chamkha (2009) analytically studied the oscillatory flow of micropolar fluid over a vertical plate embedded in a porous medium.

The ESHS process is the better heating practices due to significant enhancement in the thermal field because of slight increase in the magnitude of the heat source. Mahanthesh, Lorenzini, Oudina, and Animasaun (2019) examined the significance of exponential heat source on radiative nanofluid flow due to radially elongated disk. Nagaraja and Gireesha (2020) studied on exponential heat source aspects past a stretching sheet. Recently, Swain, Animasaun, and Ibrahim (2021) studied the influences of exponential heat source and Joule heating on water based copper and copper oxide nanofluid flow over an elongating/shrinking sheet inspired by inclined magnetic field.

The current article aims at to study the Casson nanofluid flow over a stretching sheet in a porous medium. Buongiorno model has been employed to study the influences of Brownian movement, thermophoresis, thermal radiation, magnetic field, porosity and ESHS. The novelty lies in generalized study of the Casson nanofluid model on introducing thermal radiation and permeability of porous medium which has not drawn the attention of previous researchers. The governing equations admit scaling transformation leading to introduce similarity variable concomitantly the PDEs are converted to ODEs. The obtained ODEs are solved using Runge-Kutta fourth order method accompanied by shooting technique. The physical significances of the operating parameters are explained in the text through graphs and tables.

2. Formulation of the Problem

The 2D stagnation point flow of an unsteady Casson nanoliquid over an extending sheet in a porous medium is considered. The plate is placed along *x*-axis and *y*-axis is normal to it (Figure 1). The flow is assumed to be confined to $y > 0$. Let us consider when the time $t < 0$ the fluid flow is steady. The unsteady fluid and heat flows start at $t = 0$. It is assumed that:

- There is no slip between the base fluid and suspended nanoparticles.
- The viscous dissipative heat is assumed to be negligible due to laminar flow.
- The effect of induced magnetic field is neglected due to small Reynolds number.

The rheological equation of state for an isotropic and incompressible flow of a Casson fluid (Senapati, Swain, & Parida, 2020) is expressed as

$$\tau_{ij} = \begin{cases} 2\left(\mu_B + \dfrac{p_y}{\sqrt{2\pi}}\right)e_{ij}, \pi > \pi_c \\ 2\left(\mu_B + \dfrac{p_y}{\sqrt{2\pi_c}}\right)e_{ij}, \pi < \pi_c \end{cases}$$

where $e_{ij} = \dfrac{1}{2}\left(\dfrac{\partial u_i}{\partial x_j} + \dfrac{\partial u_j}{\partial x_i}\right)$ is the rate of strain tensor, τ_{ij} is the component of stress tensor, μ_B is the Casson coefficient of viscosity, $\pi = e_{ij}e_{ij}$ is the product of the rate of strain tensor with itself, π_c is the critical value of the product of the rate of strain tensor with itself, P_y is the yield stress of the fluid.

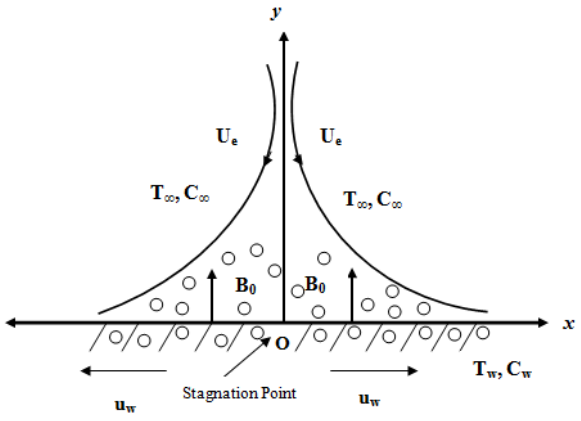

Figure 1. Flow geometry and Cartesian system

The governing equations following Rout and Mishra (2018) are given by

$$\frac{\partial u}{\partial x}+\frac{\partial v}{\partial y}=0 \tag{1}$$

$$\frac{\partial u}{\partial t}+u\frac{\partial u}{\partial x}+v\frac{\partial v}{\partial y}=\frac{\partial U_e}{\partial t}+U_e\frac{\partial U_e}{\partial x}+\upsilon_f\left(1+\frac{1}{\gamma}\right)\frac{\partial^2 u}{\partial y^2}-\frac{\sigma B_0^2}{\rho_f}(u-U_e)-\frac{\upsilon_f}{K^*}\left(u-U_e\right) \tag{2}$$

$$\begin{aligned}\frac{\partial T}{\partial t}+u\frac{\partial T}{\partial x}+v\frac{\partial T}{\partial y}=\alpha\frac{\partial^2 T}{\partial y^2}+\tau\left[D_B\frac{\partial T}{\partial y}\frac{\partial C}{\partial y}+\frac{D_T}{T_\infty}\left(\frac{\partial T}{\partial y}\right)^2\right]-\frac{1}{(\rho c)_f}\frac{\partial q_r}{\partial y}\\ +\frac{Q}{(\rho c)_f}\left(T_w-T_\infty\right)\exp\left(-\sqrt{\frac{a}{\upsilon_f(1-\lambda t)}}\,ny\right)\end{aligned} \tag{3}$$

$$\frac{\partial C}{\partial t}+u\frac{\partial C}{\partial x}+v\frac{\partial C}{\partial y}=D_B\frac{\partial^2 C}{\partial y^2}+\left(\frac{D_T}{T_\infty}\right)\frac{\partial^2 T}{\partial y^2} \tag{4}$$

with appropriate boundary conditions

$$\left.\begin{aligned}u=u_w(x,t)=\frac{ax}{1-\lambda t},v=0,T=T_w(x,t),C=C_w(x,t),\ \ at\ y=0\\ u=U_e(x,t)=\frac{bx}{1-\lambda t},T\to T_\infty,C\to C_\infty,\qquad\qquad as\ y\to\infty\end{aligned}\right\} \tag{5}$$

where $u_w\left(x,t\right)=\frac{ax}{1-\lambda t},U_e\left(x,t\right)=\frac{bx}{1-\lambda t},T_w(x,t)=T_\infty+T_0\left[\frac{ax^2}{(1-\lambda t)^{-2}}\right],\alpha=\frac{k}{\left(\rho c\right)_f}$,

$C_w(x,t)=C_\infty+C_0\left[\frac{ax^2}{(1-\lambda t)^{-2}}\right],\tau=\frac{\left(\rho c\right)_p}{\left(\rho c\right)_f}$ and T_0,C_0 are positive reference temperature and nanoparticle volume fraction respectively such that $0<T_0<T_w$ and $0<C_0<C_w$.

Using Rosseland approximation (Swain, Parida, & Dash, 2018), the radiative heat flux is given by

$$q_r=-\frac{4\sigma}{3k^*}\frac{\partial T^4}{\partial y}\Rightarrow\frac{\partial q_r}{\partial y}=-\frac{16\sigma^* T_\infty^3}{3\left(\rho c\right)_f k^*}\frac{\partial^2 T}{\partial y^2} \tag{6}$$

where σ^* is the Stefan–Boltzmann constant and k^* is the absorption coefficient such

In view of equation (6), equation (3) becomes

$$\begin{aligned}\frac{\partial T}{\partial t}+u\frac{\partial T}{\partial x}+v\frac{\partial T}{\partial y}=\alpha\ \frac{\partial^2 \mathrm{T}}{\partial y^2}+\tau\left[D_B\frac{\partial T}{\partial y}\frac{\partial C}{\partial y}+\frac{D_T}{T_\infty}\left(\frac{\partial T}{\partial y}\right)^2\right]+\frac{16\sigma^* T_\infty^3}{3\left(\rho c\right)_f k^*}\frac{\partial^2 T}{\partial y^2}\\ +\frac{Q}{(\rho c)_f}\left(T_w-T_\infty\right)\exp\left(-\sqrt{\frac{a}{\upsilon_f(1-\lambda t)}}\,ny\right)\end{aligned} \tag{7}$$

Consider the following similarity variables and transformations

$$\left.\begin{aligned}\eta=\sqrt{\frac{a}{\upsilon_f(1-\lambda t)}}\,y,\psi=\sqrt{\frac{a\upsilon_f}{(1-\lambda t)}}\,xf(\eta),\\ T=T_\infty+T_0\left[\frac{ax^2}{(1-\lambda t)^{-2}}\right]\theta(\eta),C=C_\infty+C_0\left[\frac{ax^2}{(1-\lambda t)^{-2}}\right]\phi(\eta)\end{aligned}\right\} \tag{8}$$

The stream function ψ is defined as $u=\frac{\partial\psi}{\partial y}, v=-\frac{\partial\psi}{\partial x}$, so that $u=\frac{ax}{1-\lambda t}f'(\eta)$ and $v=-\sqrt{\frac{a\upsilon_f}{1-\lambda t}}f(\eta)$. By the help of equation (8), the equations (1) – (4) become

$$\left(1+\frac{1}{\gamma}\right)f'''+ff''-f'^2-(M+K)(f'-\beta)+\beta^2-S\left(\frac{1}{2}\eta f''+f'-\beta\right)=0 \tag{9}$$

$$\left(1+\frac{4}{3}R\right)\theta''+\Pr\left[S\left(2\theta-\frac{1}{2}\eta\theta'\right)+f\theta'-f'\theta+Nb\,\theta'\phi'+Nt\,\theta'^2+Q_e\exp(-n\eta)\right]=0 \tag{10}$$

$$\phi''+Sc\left[S\left(2\phi+\frac{1}{2}\eta\phi'\right)+f\phi'-f'\phi\right]+\frac{Nt}{Nb}\theta''=0 \tag{11}$$

$$\left.\begin{aligned} &f'(\eta)=1,\ f(\eta)=0,\theta(\eta)=1,\phi(\eta)=1 \quad at\ \eta=0\\ &f'(\eta)=\beta,\theta(\eta)=0,\phi(\eta)=0 \qquad as\ \eta\to\infty \end{aligned}\right\} \tag{12}$$

where $S=\frac{\lambda}{a},\beta=\frac{b}{a},\Pr=\frac{\upsilon_f}{\alpha},R=\frac{4T_\infty^3\sigma^*}{k^*k},M=\frac{\sigma B_0^2}{\rho_f a},K=\frac{\upsilon_f}{K^*a},Nb=\frac{\tau D_B(C_w-C_\infty)}{\upsilon_f}$,

$Nt=\frac{\tau D_T(T_w-T_\infty)}{\upsilon_f T_\infty},Sc=\frac{\upsilon_f}{D_B}$.

The skin friction coefficient C_f, the local Nusselt number Nu_x and the local Sherwood number Sh_x which are defined as follows

$$C_f=\frac{\mu}{\rho_f U_w^2}\left(\frac{\partial u}{\partial y}\right)_{y=0}\Rightarrow \mathrm{Re}_x^{0.5}C_f=f''(0) \tag{13}$$

$$Nu=\frac{-x}{(T_w-T_\infty)}\left[\frac{\partial T}{\partial y}-\frac{4\sigma^*}{3k'^*}\left(\frac{\partial T^4}{\partial y}\right)\right]_{y=0}\Rightarrow \mathrm{Re}_x^{-0.5}Nu_x=-\left(1+\frac{4}{3}R\right)\theta'(0) \tag{14}$$

$$Sh=\frac{-x}{(C_w-C_\infty)}\left(\frac{\partial C}{\partial y}\right)_{y=0}\Rightarrow \mathrm{Re}_x^{-0.5}Sh_x=-\phi'(0) \tag{15}$$

where $\mathrm{Re}_x=\frac{u_w x}{\upsilon_f}$ is the local Reynolds number.

3. Results and Discussion

The set of non-linear coupled ODEs (9) – (12) are solved numerically using shooting technique with MATLAB code having step length $\Delta\eta=0.01$ and error tolerance 10^{-5}. During calculation, we fix the parameters as Pr = *n* = 2. *Sc* = 1, *M* = *K* = γ = β = 0.5, *S* = *Nb* = *Nt* = 0.3, *R* = Q_e = 0.1 unless otherwise mentioned. To check the validity of our results with previous works of Das *et al.*, (2014), Rout and Mishra (2018) and Swain *et al.*, (2017), the values of *f''*(0) are calculated for β with *Nb* = *Nt* = 0, $\gamma \to \infty$ (Newtonian fluid), *S* = 0 (steady flow), *R* = Q_e = 0 (Table 1).

From Figure 2 it is interesting to note that significant effect of stretching ratio parameter (β) on horizontal component of velocity *f'*(η) with the distance from the bounding surface, η. It is seen that when $\beta > 1$ i.e. the rate of stretching has predominance over plate stretching then the flow has a boundary layer structure otherwise there exist an inverted boundary layer structure ($\beta < 1$). For fixed values of *a* (corresponding to plate stretching), the increase in *b* implies increase in straining motion near the stagnation region resulting in increased acceleration of the free stream. This leads to thinning of boundary layer with increasing in β. It is also to note that $\beta < 1$, there is an inverted boundary layer structure. This means that when plate stretching velocity exceeds the rate of free stream stretching the inverted boundary layer is formed. Further, it is to note that magnetic parameter increases the horizontal velocity and permeability of the medium decreases it for boundary layer structure. For inverted structure, reverse effects of these parameters are marked. It is really a noteworthy observation that magnetic parameter increases the horizontal component of velocity, usually, the magnetic parameter imbibes a mechanical force (Lorentz force), which resists the flow along the main direction. In the present case the effect is reversed. Of course, in inverted boundary layer, the magnetic parameter decreases the velocity. A physical reasoning may be attributed to an increase is that the increase in straining motion due to stretching generated over power the resistive force due to interaction of transverse magnetic field with that of electrically conducting fluid. Figure 3 depicts the effect of unsteady parameter (*S*). An increase in *S* implies increase in λ.

Table 1. Comparison of $f''(0)$ for different values of β when $M = K = S = Q_e = 0$, $\gamma \rightarrow \infty$.

β	$f''(0)$			
	Das *et al.*, (2014)	Swain *et al.*, (2017)	Rout and Mishra (2018)	Present study
0.1	-0.969328	-0.96965625	-0.96966	-0.9696514
0.2	-0.918098	-0.91816450	-0.91816	-0.9181601
0.5	-0.667301	-0.66726432	-0.66726	-0.6672609
2	2.017467	2.01750252	2.017502	2.0175025
3	4.729406	4.72928082	---	4.7292808

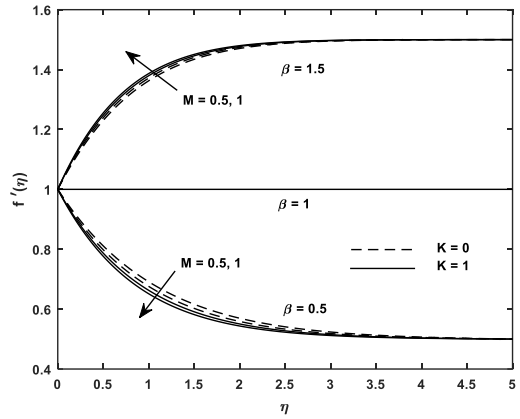

Figure 2. Velocity profiles for various values of M, K and β

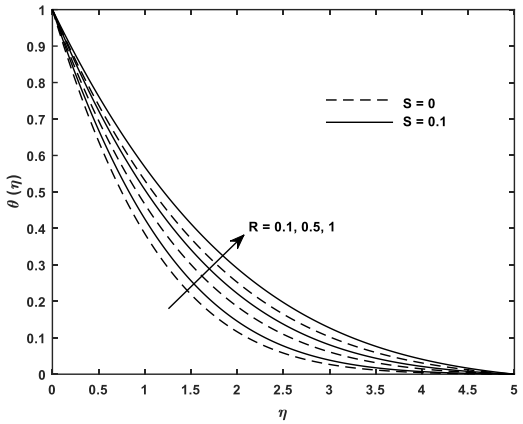

Figure 4. Temperature profiles for various values of R and S

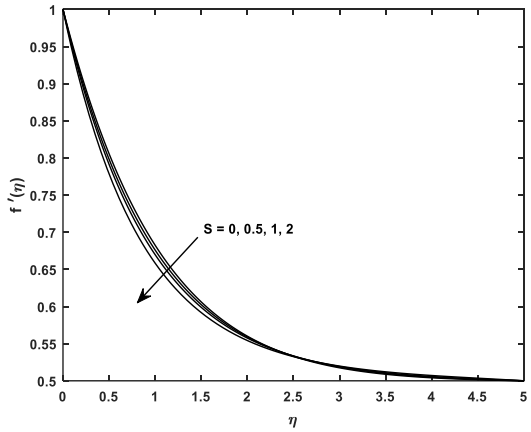

Figure 3. Velocity profiles for various values of S

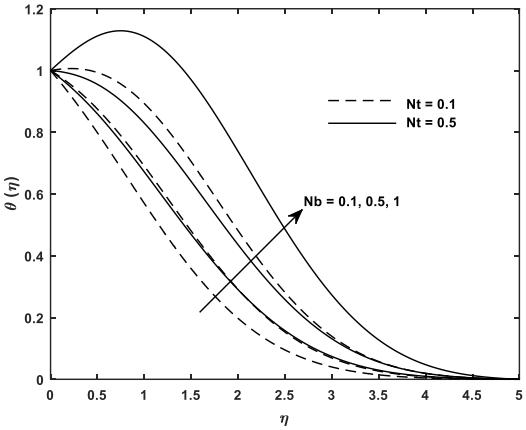

Figure 5. Temperature profiles for various values of Nb and Nt

For fixed value of a, which contributes to increasing unsteadiness. It is seen that an increase in S slightly decreases the velocity in the flow domain.

From Figure 4 it is observed that unsteady parameter increases the temperature of the flow domain and it is further enhanced by the radiation parameter (R). From Figure 5 it is seen that thermophoresis parameter (Nt) decreases the temperature but Brownian motion parameter (Nb) increases the temperature throughout the domain. The thermophoresis is the thermal process which is the ratio of thermal diffusion and momentum diffusion through kinematic viscosity (v). Thus, an increase in Nt for a fixed v, implies increase in the process of thermo diffusion. Therefore, increase in Nt increases the temperature in the flow domain. One interesting point is to note that for Nt = 0.5, higher diffusion, the temperature exceeds the prescribed temperature at the plate surface which is vital. Hence, care should be taken to regulate the thermal diffusion to avoid the thermal instability. Figure 6 shows that an increase in exponential index (n) decreases the thermal power. It is evident from the last term of equation (3). Hence, an increase in n results the decrease of temperature. Figure 7 shows that an increase in strength of temperature dependent heat source leads to increase the temperature of the fluid layer.

Figure 8 displays the concentration distribution for various values of Sc and S. It is observed that higher values of Sc (heavier species) leads to lower the concentration level but higher values of S, for a fixed value of v, leads to increase the concentration level at all the layers. Figure 9 depicts the effects of Brownian motion parameter (Nb) and thermophoresis parameter (Nt) on concentration distribution. It is observed that an increase in Brownian motion reduces the

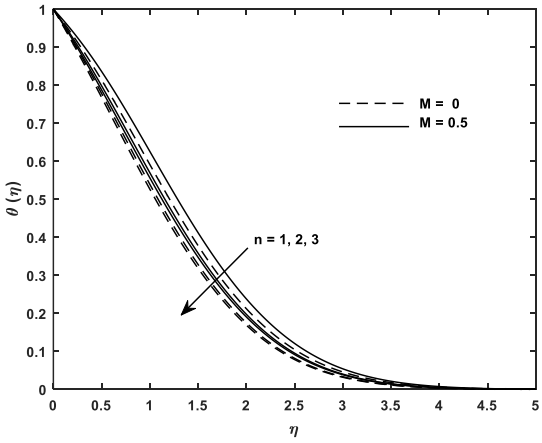

Figure 6. Temperature profiles for various values of *M* and *n*

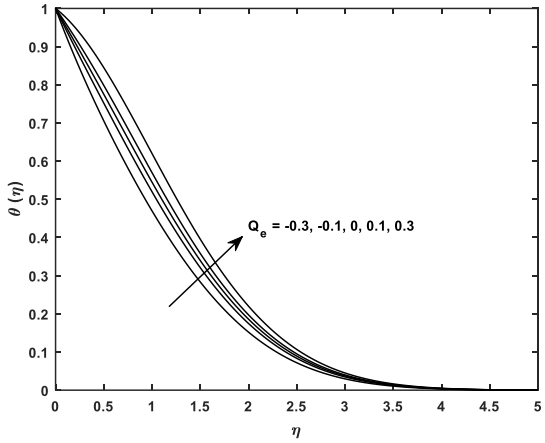

Figure 7. Temperature profiles for various values of Q_e

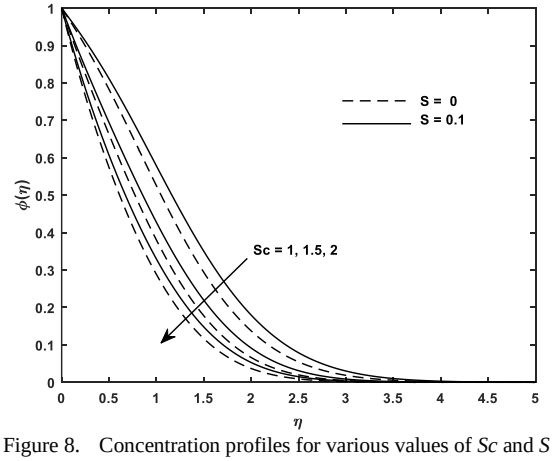

Figure 8. Concentration profiles for various values of *Sc* and *S*

concentration profiles whereas thermophoresis parameter increases the mass transfer leading to higher concentration. This remark is supported by thermo diffusion (Schlichting, and Gersten (2000)).

Figure 10 displays the velocity, temperature and concentration distribution for different values of Casson parameter (γ). When $\gamma \rightarrow \infty$, the model reduces to Newtonian viscous fluid model. Therefore, higher values of γ leads to less of Casson fluidity. It is observed that an increase in γ, leads to decrease the velocity but increases both temperature and

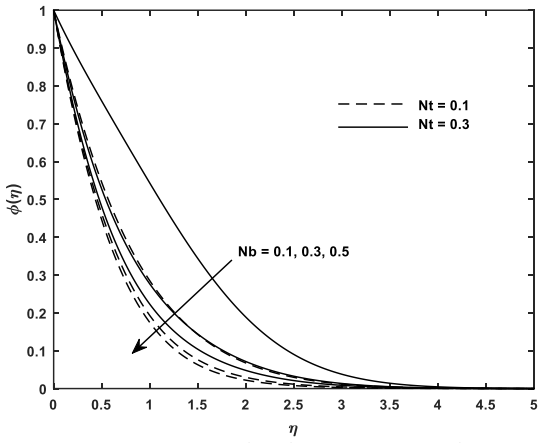

Figure 9. Concentration profiles for various values of *Nb* and *Nt*

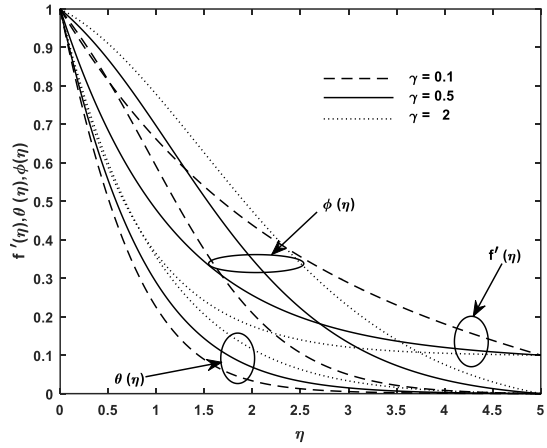

Figure 10. Velocity, temperature and concentration profiles for various values of γ when $\beta = 0.1$

concentration distribution in the flow domain. In other words, decreas in γ reversed effects are observed. Thus, the more of Casson fluidity enhances the momentum diffusion in the flow domain but reduces the thermal and mass diffusion asymptotically when coupling parameter β ($\beta < 1$) i.e. under the predominance of free stream stretching. Therefore, it is suggested to regulate the Casson parameter to attain the required level of concentration.

An overall observation from Table 2, it is noted that the skin friction coefficient remains negative always except two cases when $\beta = 1.2, 1.5$, where it assumes positive values. The reason is evident from the velocity distribution (structure of boundary layer). Heat transfer coefficient (Nusselt number) is always positive indicating heat flows from the plate to fluid as long as $T_w > T_\infty$. The Sherwood number remains positive for *Sc=1* and for low values of Schmidt number it becomes negative. Hence, mass transfer coefficient depends upon the parametric effect enumerated in the table. Moreover, Table 2 displays the numerical values of surface criteria, which controls the process of momentum, thermal and mass diffusion in the boundary layers. In the present study, it is seen that the force coefficient decreases with an increase in *M* and $\beta < 1$. The physical attribution runs as: reduction of velocity with increase in *M* is attributed less shearing effect at the bounding surface. Hence, skin friction decreases. Similar explanation can be given in case of $\beta > 1$ and *S* where skin

Table 2. Computation of $f''(0), -\theta'(0)$ and $-\phi'(0)$ when $K = \gamma = 0.5$, $Nb = Nt = 0.1$, $n = 2$

M	β	S	Pr	R	Sc	Q_e	$f''(0)$	$-\theta'(0)$	$-\phi'(0)$
0	0	0	1	0.1	1	0	-1.339497	0.917426	0.609191
0.5	0						-0.817786	1.043507	0.521385
	0.3						-0.634473	1.111413	0.598927
	0.5						-0.480497	1.154215	0.643419
	1.2						0.226260	1.293905	0.774583
	1.5						0.598392	1.349797	0.823529
	0.5	0.3					-0.498855	0.761924	0.392714
		0.5					-0.510865	0.225037	0.076172
			2				-0.510865	0.483172	-0.191402
			5				-0.510865	1.045874	-0.625184
				0.3			-0.510865	1.110847	-0.512791
				0.5			-0.510865	1.156090	-0.426788
					0.78		-0.510865	1.184018	-0.494103
					0.6		-0.510865	1.199796	-0.512427
						0.3	-0.510865	0.563060	-0.144689
						0.1	-0.510865	0.987657	-0.389913
						0	-0.510865	1.199796	-0.512427
						-0.1	-0.510865	1.411827	-0.634877
						-0.3	-0.510865	1.835569	-0.879581

friction increases with increase in β and S. The rate of heat transfer increases with increase in M, R, Pr, Q_e and β on the other hand reverse effect is observed in case of S and Sc.

4. Conclusions

From the present study the following conclusions are drawn:

- The more of Casson fluidity enhances the momentum diffusion in the flow domain and reduces the thermal and mass diffusion processes.
- The ratio of free stream stretching to plate stretching affects significantly the shearing stress at the plate to alter the sign of the skin friction.
- When the rate of plate stretching velocity exceeds the rate of free stream stretching the inverted boundary layer is formed otherwise flow phenomena possesses a boundary layer structure.
- It is interesting to note that magnetic parameter increases the horizontal component of velocity in the domain of boundary layer structure.
- The temperature distribution exceeds the prescribed temperature at the plate surface for higher diffusion. Hence, care should be taken to regulate the thermal diffusion to avoid the thermal instability.
- Higher values of S and Nt lead to increase the concentration level in all the layers whereas Nb reduces it.

References

Abd El-Aziz, M. & Afify, A.A. (2019). Effect of Hall current on MHD slip flow of Casson nanofluid over a stretching sheet with zero nanoparticle mass flux. *Thermophysics and Aeromechanics*, *26*, 429-443. doi:10.1134/S0869864319030119

Abd El-Aziz, M. & Afify, A. A. (2019). MHD casson fluid flow over a stretching sheet with entropy generation analysis and hall influence. *Entropy*, *21*, 592. doi:10.3390/e21060592

Abel, M. S., Mahesha, N. & Tawade, J. (2009). Heat transfer in a liquid film over an unsteady stretching surface with viscous dissipation in presence of external magnetic field. *Applied Mathematical Modelling*, *33*, 3430-3441. doi:10.1016/j.apm.2008.11.021

Bhandari, A. (2019). Radiation and chemical reaction effects on nanofluid flow over a stretching sheet. *Fluid Dynamics and Materials Processing*, *15*, 557-582. doi:10.32604/fdmp.2019.04108

Buongiorno, J. (2006). Convective transport in nanofluids. *ASME Journal of Heat Transfer*, *128*, 240-250. doi:10.1115/1.2150834

Casson, N. (1959). A flow equation for pigment oil suspensions of printing ink type. In C. C. Mill (Ed.), *Rheology of Dispersed System (*pp.84-102), Oxford, England: Pergamon Press.

Chamkha, A. J. (1997). MHD-free convection from a vertical plate embedded in a thermally stratified porous medium with Hall effects. *Applied Mathematical Modelling*, 21, 603-609.

Chamkha, A. J. (1997). Hydromagnetic natural convection from an isothermal inclined surface adjacent to a thermally stratified porous medium. *International Journal of Engineering Science*, 10/11, 975-986. doi:10.1016/S0020-7225(96)00122-X

Chamkha, A. J. (2000). Thermal radiation and buoyancy effects on hydromagnetic flow over an accelerating permeable surface with heat source or sink. *International Journal of Engineering Science*, *38*, 1699-1712.

Chamkha, A. J., Dogonchi, A. S. & Ganji, D. D. (2019). Magneto-hydrodynamic flow and heat transfer of a hybrid nanofluid in a rotating system among two surfaces in the presence of thermal radiation and Joule heating. *AIP Advances*, *9*, 025103. doi:10.1063/1.5086247

Chamkha, A. J. & Khaled, A. R. A. (2000). Hydromagnetic combined heat and mass transfer by natural convection from a permeable surface embedded in a fluid- saturated porous medium. *International Journal of Numerical Methods for Heat and Fluid*

Flow, *10*, 455-476.

Chamkha, A. J. & Mohamed, R. A. (2011). Unsteady MHD natural convection from a heated vertical porous plate in a micropolar fluid with Joule heating, chemical reaction and radiation effects. *Meccanica*, *46*, 399-411. doi:10.1007/s11012-010-9321-0

Choi, S. U. S. (1995). Enhancing thermal conductivity of the fluids with nanoparticles. *ASME Fluids Engineering Division*, *231*, 99-105.

Daniel, Y. S., Aziz, Z. A., Ismail, Z. & Salah, F. (2019). Thermal radiation on unsteady electrical MHD flow of nanofluid over stretching sheet with chemical reaction. *Journal of King Saud University-Science*, *31*, 804-812. doi:10.1016/j.jksus.2017.10.002

Das, M., Mahanta, G., Shaw, S. & Parida, S. B. (2019). Unsteady MHD chemically reactive double-diffusive Casson fluid past a flat plate in porous medium with heat and mass transfer. *Heat Transfer-Asian Research*, *48*, 1761-1777. doi:10.1002/htj.21456

Das, K., Duari, P. R. & Kundu, P. K. (2014). Nanofluid flow over an unsteady stretching surface in presence of thermal radiation. *Alexandria Engineering Journal*, *53*, 737-745. doi:10.1016/j.aej.2014.05.002

Ganesh, K. K., Reddy, M. G., Sudharani, M. V. V. N. L., Shehzad, S. A. & Chamkha, A. J. (2020). Cattaneo-Christov heat diffusion phenomenon in Reiner-Philippoff fluid through a transverse magnetic field. *Physica A*, *541*, 123330. doi:10.1016/j.physa.2019.123330

Goyal, M. & Bhargava, R. (2018). Simulation of natural convective boundary layer flow of a nanofluid past a convectively heated inclined plate in the presence of magnetic field. *International Journal of Applied and Computational Mathematics*, *63*, 1-24. doi:10.1007/s40819-018-0483-0

Hsiao. K. L. (2016). Stagnation electrical MHD nanofluid mixed convection with slip boundary on a stretching sheet. *Applied Thermal Engineering*, *98*, 850-861. doi:10.1016/j.applthermaleng.2015.12.138

Ibrahim, W. (2015). Nonlinear radiative heat transfer in magnetohydrodynamic (MHD) stagnation point flow of nanofluid past a stretching sheet with convective boundary condition. *Propulsion and Power Research*, *4*, 230-239. doi:10.1016/j.jppr.2015.07.007

Ibrahim, S. M., Kumar, P. V., Lorenzini, G. & Lorenzini, E. (2019). Influence of joule heating and heat source on radiative MHD flow over a stretching porous sheet with power-law heat flux. *Journal of Engineering Thermophysics*, *28*, 332-344. doi:10.1134/S1810232819030044

Khedr, M. E. M., Chamkha, A. J. & Bayomi, M. (2009). MHD flow of a micropolar fluid past a stretched permeable surface with heat generation or absorption. *Nonlinear Analysis: Modelling and Control*, *14*, 27-40.

Krishna, M. V. & Chamkha, A. J. (2019). Hall and ion slip effects on MHD rotating boundary layer flow of nanofluid past an infinite vertical plate embedded in a porous medium. *Results in Physics*, *15*, 102652. doi:10.1016/j.rinp.2019.102652

Krishna, M. V., Ahamad, N. A. & Chamkha, A. J. (2020). Hall and ion slip effects on unsteady MHD free convective rotating flow through a saturated porous medium over an exponential accelerated plate. *Alexandria Engineering Journal*, *59*, 565-577. doi:10.1016/j.aej.2020.01.043

Krishna, M. V. & Chamkha, A. J. (2020). Hall and ion slip effects on MHD rotating flow of elastico-viscous fluid through porous medium. *International Communications in Heat and Mass Transfer*, *113*, 104494. doi:10.1016/j.icheatmasstransfer.2020.104494

Krishna, M. V., Ahamad, N. A. & Chamkha, A. J. (2021). Hall and ion slip impacts on unsteady MHD convective rotating flow of heat generating/absorbing second grade fluid. *Alexandria Engineering Journal*, *60*, 845-858. doi:10.1016/j.aej.2020.10.013

Krishnan, B. C., Rittgers, S. E., & Yoganathan, A. P. (2012). *Biofluid mechanics: The human circulation* (2nd ed.). New York, NY: Taylor and Francis.

Mahanthesh, B., Lorenzini, G., Oudina, F. M. & Animasaun, I. L. (2019). Significance of exponential space-and thermal-dependent heat source effects on nanofluid flow due to radially elongated disk with Coriolis and Lorentz forces. *Journal of Thermal Analysis and Calorimetry*, *141*, 37-44. doi:10.1007/s10973-019-08985-0

Modather, M., Rashad, A. M. & Chamkha, A. J. (2009). An analytical study of MHD heat and mass transfer oscillatory flow of a micropolar fluid over a vertical permeable plate in a porous medium. *Turkish Journal of Engineering and Environmental Sciences*, *33*, 245-257. doi:10.3906/muh-0906-31

Nagaraja, B. & Gireesha, B. J. (2020). Exponential space-dependent heat generation impact on MHD convective flow of Casson fluid over a curved stretching sheet with chemical reaction. *Journal of Thermal Analysis and Calorimetry*, *143*, 4071-4079. doi:10.1007/s10973-020-09360-0

Oyelakin, I. S., Mondal, S. & Sibanda, P. (2016). Unsteady Casson nanofluid flow over a stretching sheet with thermal radiation, convective and slip boundary conditions. *Alexandria Engineering Journal*, *55*, 1025-1035. doi:10.1016/j.aej.2016.03.003

Pal, D., Mandal, G. & Vajravalu, K. (2015). Mixed convection stagnation-point flow of nanofluids over a stretching/shrinking sheet in a porous medium with internal heat generation/absorption. *Communications in Numerical Analysis*, *1*, 30-50. doi:10.5899/2015/cna-00228

Reddy, P. S. & Chamkha, A. J. (2016). Soret and Dufour effects on MHD convective flow of Al_2O_3–water and TiO_2–water nanofluids past a stretching sheet in porous media with heat generation/absorption. *Advanced Powder Technology*, *27*, 1207-1218. doi:10.1016/j.apt.2016.04.005

Reddy, M. G., Padma, P. & Shankar, B. (2015). Effects of viscous dissipation and heat source on unsteady MHD flow over a stretching sheet. *Ain Shams Engineering Journal*, *6*, 1195-1201. doi:10.1016/j.asej.2015.04.006

Rout, B. C. & Mishra, S. R. (2018). Thermal energy transport on MHD nanofluid flow over a stretching surface: A comparative study. *Engineering Science and Technology, an International Journal*, 21, 60-69. doi:10.1016/j.jestch.2018.02.007

Schlichting, H. & Gersten, K. (2000). *Boundary layer theory* (8th ed.). New York, NY: Springer-Verlag.

Senapati, M., Parida, S. K., Swain, K. & Ibrahim, S. M. (2020). Analysis of variable magnetic field on chemically dissipative MHD boundary layer flow of Casson fluid over a nonlinearly stretching sheet with slip conditions. *International Journal of Ambient Energy*. doi:10.1080/01430750.2020.1831601

Senapati, M., Swain, K. & Parida, S. K. (2020). Numerical analysis of three-dimensional MHD flow of Casson nanofluid past an exponentially stretching sheet. *Karbala International Journal of Modern Science*, *6*(1), 93-102. doi:10.33640/2405-609X.1462

Seyedi, S. H., Saray, B. N. & Chamkha, A. J. (2020). Heat and mass transfer investigation of MHD Eyring–Powell flow in a stretching channel with chemical reactions. *Physica A*, 544, 124109. doi:10.1016/j.physa.2019.124109

Sreedevi, P., Reddy, P. S. & Chamkha, A. J. (2020). Heat and mass transfer analysis of unsteady hybrid nanofluid flow over a stretching sheet with thermal radiation. *SN Applied Sciences*. doi:10.1007/s42452-020-3011-x

Swain, K., Animasaun, I. L. & Ibrahim, S. M. (2021). Influence of exponential space-based heat source and Joule heating on nanofluid flow over an elongating/shrinking sheet with an inclined magnetic field. *International Journal of Ambient Energy*. doi:10.1080/01430750.2021.1873854

Swain, K., Parida, S. K. & Dash, G. C. (2018). Effects of non-uniform heat source/sink and viscous dissipation on MHD boundary layer flow of Williamson nanofluid through porous medium. *Defect and Diffusion Forum*, *389*, 110-127. doi:10.4028/www.scientific.net/DDF.389.110

Swain, K., Parida, S. K. & Dash, G. C. (2017). MHD heat and mass transfer on stretching sheet with variable fluid properties in porous medium. *AMSE, Modelling B*, *86*(4), 864-884. doi:10.18280/mmc_b.860404

Takhar, H. S., Chamkha, A. J. & Nath, G. (2002). MHD flow over a moving plate in a rotating fluid with magnetic field, Hall currents and free stream velocity. *International Journal of Engineering Science*, *40*, 1511-1527.

Takhar, H. S., Chamkha, A. J. & Nath, G. (1999). Unsteady flow and heat transfer on a semi-infinite flat plate with an aligned magnetic field. *International Journal of Engineering Science*, *37*, 1723-1736.

Wakif, A., Chamkha, A., Animasaun, I. L., Zaydan, M., Waqas, H. & Sehaqui, R. (2020). Novel physical insights into the thermodynamic irreversibilities within dissipative EMHD fluid flows past over a moving horizontal riga plate in the coexistence of wall suction and joule heating effects: A comprehensive numerical investigation. *Arabian Journal for Science and Engineering*. doi:10.1007/s13369-020-04757-3

Appendix

Nomenclature

u, v	Velocities along x and y directions respectively
a	Stretching rate
b	Strength of stagnation flow
t	Time
B_0	Magnetic field strength
M	Magnetic parameter
K	Porosity parameter
n	Exponential index
Pr	Prandtl number
Nb	Brownian motion parameter
Nt	Thermophoresis parameter
Sc	Schmidt number
R	Radiation parameter
S	Unsteadiness parameter
D_B	Brownian diffusion coefficient
k	Thermal conductivity coefficient
D_T	Thermophoresis diffusion coefficient
C_P	Specific heat at constant temperature
$(\rho c)_p$	Heat parameter of nanoparticle
$(\rho c)_f$	Heat parameter of base fluid
K^*	Permeability of the medium
Q	Heat source/ sink coefficient
Q_e	Exponential space-based heat source/ sink parameter
T	Temperature
C	Concentration
U_e	Ambient fluid velocity
T_w	Temperature of the wall
T_∞	Ambient temperature
C_∞	Ambient concentration
	Greek Symbols
η	Similarity variable
σ	Electrical conductivity
ψ	Stream function
λ	Positive rate constant
γ	Casson parameter
β	Stretching ratio parameter
α	Thermal diffusivity
τ	Ratio of the nanoparticle heat capacity to the base fluid heat capacity
μ_f	Dynamic viscosity of base fluid
υ_f	Kinematic viscosity of base fluid
ρ_f	Density of base fluid